

EXPERIMENTAL AND NUMERICAL STUDY OF STRENGTH PREDICTION OF COLD FORGED PARTS BASED ON THE CHABOCHE COMBINED HARDENING MODEL

YASUHARU SHINKAI^{*}, OSAMU KADA^{*}, RYUICHI NISHIMURA[†],
HIROKI NARUMIYA^{*} AND NOBUO YOSHIKAWA[‡]

^{*} Steel Research Laboratories, R&D Laboratories, Nippon Steel Corporation
20-1 Shintomi, Futtsu, Chiba 293-8511, Japan
E-mail: shinkai.45k.yasuharu@jp.nipponsteel.com
Web page: <https://www.nipponsteel.com/en/>

[†] Steel Research Laboratories, R&D Laboratories, Nippon Steel Corporation
1-8 Fuso-cho, Amagasaki, Hyogo 660-0891, Japan

[‡] Kyushu R&D Lab., R&D Laboratories, Nippon Steel Corporation
1-1 Tobihata-cho, Tobata-ku, Kitakyushu, Fukuoka 804-8501, Japan

Key words: Cold Forging, Bauschinger Effect, Chaboche Model, Simple Shear Tests.

Abstract. The high manufacturing costs of heat-treated cold forged parts has necessitated the possible elimination of the heat treatment process for improving their mechanical properties. In such a scenario, the strength of the parts can be determined by the degree of work hardening during cold forging; moreover, optimizing the shapes of cold forged parts based on strength prediction via finite element analysis (FEA) can assist in realizing the weight reduction of these parts as well as the cost reduction. However, when the parts are subjected to tensile loads during operation in the opposite direction of compressive loads imposed during cold forging (the Bauschinger effect), predicting the strength of these parts using an isotropic hardening model is inappropriate because it overestimates their strength. Only a few studies have reported on FEA models that consider the influence of the Bauschinger effect in the field of bulk forming.

In this study, a strength prediction method using a Chaboche combined hardening model was investigated for predicting the strength of cold forged parts that are not subjected to heat treatment after cold forging. Simple shear tests were performed to obtain stress–strain curves with reversed loading over a wide range of strains. The simple shear tests facilitated the accurate prediction of the strength of the cold forged parts.

1 INTRODUCTION

Cold forged parts are typically subjected to heat treatment for improving their mechanical properties, especially surface hardness. However, it is favorable to omit the heat treatment process to reduce their manufacturing costs. The strength of cold forged parts in this scenario

can be determined by the degree of work hardening during cold forging; the optimization of their shapes based on strength prediction via finite element analysis (FEA) can assist in realizing the weight reduction of these parts as well as the cost reduction.

Cold forged parts are subjected to compressive loads in the process of cold forging. However, the Bauschinger effect is manifested when these parts are frequently exposed to tensile loads in the opposite direction of compressive loads during their operation. FEA with an isotropic hardening model is generally used in the field of bulk forming; however, this model does not account for the Bauschinger effect. The use of the isotropic hardening model for strength prediction results in the strength of the parts being overestimated when the Bauschinger effect occurs. Although the influence of the Bauschinger effect has been considered in springback analyses in the field of sheet forming, there have been only a few reports in the field of bulk forming^[1]. One of the reasons for this involves the difficulty in obtaining stress–strain curves with reversed loading over a wide range of strains, because of buckling, for application in the FEA of bulk forming.

A strength prediction method using a Chaboche combined hardening model^[2] was investigated in this study for predicting the strength of cold forged parts that are not subjected to heat treatment after cold forging.

2 EXPERIMENTAL AND NUMERICAL PROCEDURE

2.1 Evaluation of the strength of upset specimens

The process of evaluating the strength of cold forged parts was simplified by performing two tests, (A) and (B) (Figure 1). Cylindrical specimens were upset in test (A), following which tensile tests were performed in test (B) using specimens cut from the upset specimens. Test (A) represents the cold forging process, and test (B) corresponds to the process of evaluating the strength of cold forged parts that are subjected to tensile loads during their operation.

JIS G4051 S10C and S55C, which represent 0.10%-C and 0.55%-C carbon steels, respectively, were used as the test materials. The as-rolled round bars of S10C and S55C were normalized and spheroidized. Cylindrical specimens with a diameter of 56 mm and a height of L_0 (50, 80 mm) were cut from the round bars for test (A). The 50-mm and 80-mm tall specimens were upset to 40 mm and 50 mm, respectively; these corresponded to upsetting ratios of 20.0% and 37.5%, respectively. The upsetting tests were performed using a mechanical servo press driven by an AC servo motor. The loading rate of upsetting was quasi-static with crank motion control. The displacement rate of the slide was less than 0.5 mm/s during the process of upsetting the specimens. Lubricating oil was applied to the contact surface of the specimen and dies to facilitate upsetting.

Tensile specimens for test (B) were cut from the upset specimens, as shown in Figure 1. The tensile tests were performed at a constant crosshead displacement rate of 0.6 mm/min.

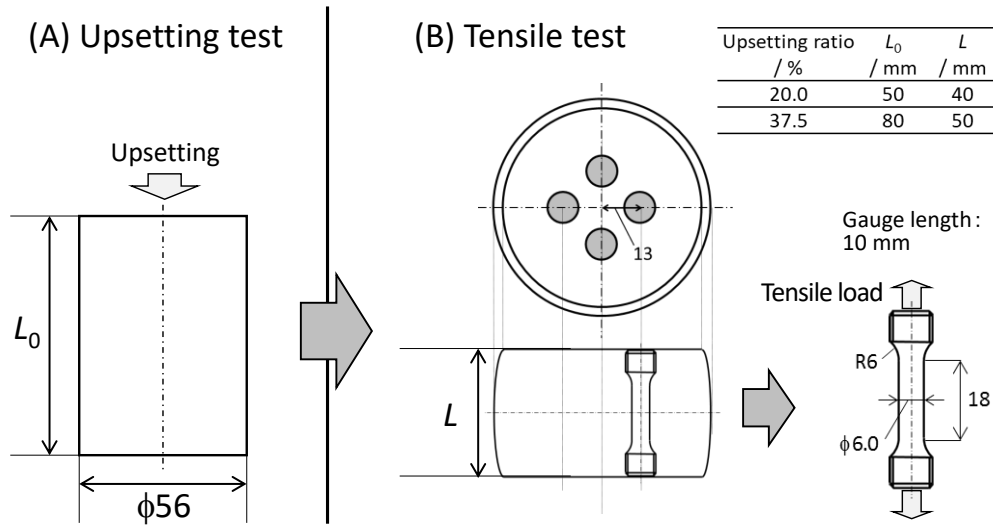


Figure 1: Schematics of the upset specimens used for the strength evaluation

2.2 FEA for predicting the strength of upset specimens

A three-dimensional FEA model that considered the Bauschinger effect was implemented to predict the load–displacement response of test (B). A Chaboche combined hardening model was used to represent the constitutive relations in the analysis. This model, which consists of a Swift isotropic hardening model and a Chaboche kinematic hardening model^[2], is expressed as follows:

$$Y = K (\bar{\varepsilon} + \varepsilon_0)^n \quad (1)$$

$$\boldsymbol{\alpha} = \sum_i^3 \boldsymbol{\alpha}_i \quad (i = 1, 2, 3) \quad (2)$$

$$d\boldsymbol{\alpha}_i = \frac{2}{3} c_i d\boldsymbol{\varepsilon}^p - \gamma_i \boldsymbol{\alpha}_i d\bar{\varepsilon} \quad (3)$$

where Y is the yield stress, $\boldsymbol{\alpha}$ is the back stress, $\boldsymbol{\alpha}_i$ is the i -th component of the back stress, $\boldsymbol{\varepsilon}^p$ is the plastic strain, and $\bar{\varepsilon}$ is the equivalent plastic strain. $K, \varepsilon_0, n, c_i, \gamma_i$ represent the material parameters. The von Mises yield function was used as the yield criterion, and the plastic flow was assumed to be associative.

Model geometries of the specimens in tests (A) and (B) were created according to Figure 1. The upper and lower dies employed for upsetting in test (A) were modeled as rigid bodies, and the specimens used in tests (A) and (B) were modeled as elastoplastic bodies and were discretized using hexahedral elements with an approximate size of 1 mm and 0.5 mm, respectively. Considering the symmetry of the model, one-eighth of the specimen in test (A) and half of the specimen in test (B) were used. The friction between the dies and the specimen was assumed to be governed by the Coulomb friction law with a coefficient of friction of 0.04, which was determined based on the shape of the upset specimen.

The simulations were carried out using the commercial finite element code Simufact Forming v15, and the Chaboche combined hardening model was implemented using its user subroutine. The effect of temperature during plastic deformation was not considered. FEA with the isotropic hardening model was also performed for enabling comparison with that of the Chaboche combined hardening model. The accuracy of the strength prediction was evaluated by comparing the calculated load–displacement curves with the experimental load–displacement curves obtained via test (B).

2.3 Simple shear tests for the identification of material parameters

Stress–strain curves were obtained using simple shear tests^[3–5] to identify the material parameters of the aforementioned constitutive relations. The geometry of the simple shear tests is shown in Figure 2. The specimens used in the single and series simple shear tests were 30 mm and 38 mm long, respectively. In the series tests, the non-uniformly-deformed ends of specimens obtained from the simple shear tests were cut, and simple shear tests were repeated. The specimens were cut at a location corresponding to a quarter of the diameter in the radial direction of bars made of the test materials so that the shear direction of the specimens is parallel to the longitudinal direction of the bars.

In a simple shear test, a 2-mm-wide area located in the center of the specimen in the transverse direction was subjected to shear by clamping the upper and lower sides of the area and moving one side in the longitudinal direction while fixing the other side. Images of a straight line drawn at the center of the specimen in the longitudinal direction were captured using a CCD camera. The shear strain in the deformed area was calculated using the change in inclination of the straight line. The shear force was measured using a load cell attached to a jig of a simple shear test apparatus, and the shear stress was calculated by dividing the shear force by the cross-sectional area of the specimen along the longitudinal direction.

The stress–strain (τ - γ^p) curve obtained from the simple shear test was transformed into an equivalent stress–strain curve ($\bar{\sigma}$ - $\bar{\epsilon}$) using the work conjugate relation^[5].

$$\bar{\sigma} = \kappa \tau \quad (4)$$

$$d\bar{\epsilon} = \frac{1}{\kappa} d\gamma^p \quad (5)$$

A constant κ was determined so that the equivalent stress–strain curves obtained as described above were in agreement with the stress–strain curves obtained from tensile tests.

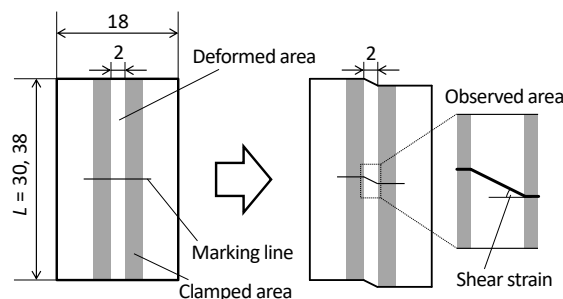


Figure 2: Geometry of specimens used in the simple shear tests

3 RESULTS AND DISCUSSION

3.1 Parameter fitting to the overall region of stress–strain curves (Case 1)

The equivalent stress–strain curves obtained from the simple shear tests are shown in Figure 3. The equivalent stress has a positive or negative sign to express the direction of loading in a convenient manner. Material parameters were identified to minimize the residual sum of squares of the experimental and calculated values of stress at each value of strain. Essentially, the parameters were obtained in a manner that ensured agreement between the calculated stress–strain curves and the overall region of the experimental stress–strain curves. The FEA conducted using these parameters is referred to as Case 1.

The load–displacement curves obtained from test (B) are shown in Figure 4. In the FEA model with isotropic hardening, necking of the tensile specimen is observed to occur immediately after plastic deformation starts, followed by a decrease in load. This deformation behavior is different from that observed in the experiments. On the other hand, the FEA model with Chaboche combined hardening shows a gradual increase in load from the beginning of the tensile test to the maximum load point, followed by a decrease in load; this deformation behavior is similar to that observed in the experiments.

The relative errors of the calculated maximum load values with respect to the experimental values in Case 1 are shown in Figure 5. The maximum load was used as an index of the strength of the upset specimens. A relative error with a positive or negative value indicates that the strength of the upset specimen has been overestimated or underestimated, respectively. The strength of the upset specimens is overestimated in the FEA model with isotropic hardening, indicating its unsuitability for strength prediction. However, the strength of the upset specimens is underestimated in the FEA model with Chaboche combined hardening, indicating its appropriateness. Nonetheless, the absolute values of relative errors corresponding to the maximum load in test (B) of the 20.0%-upset S10C specimens and the 37.5%-upset specimens exceed 10%, implying a poor prediction accuracy.

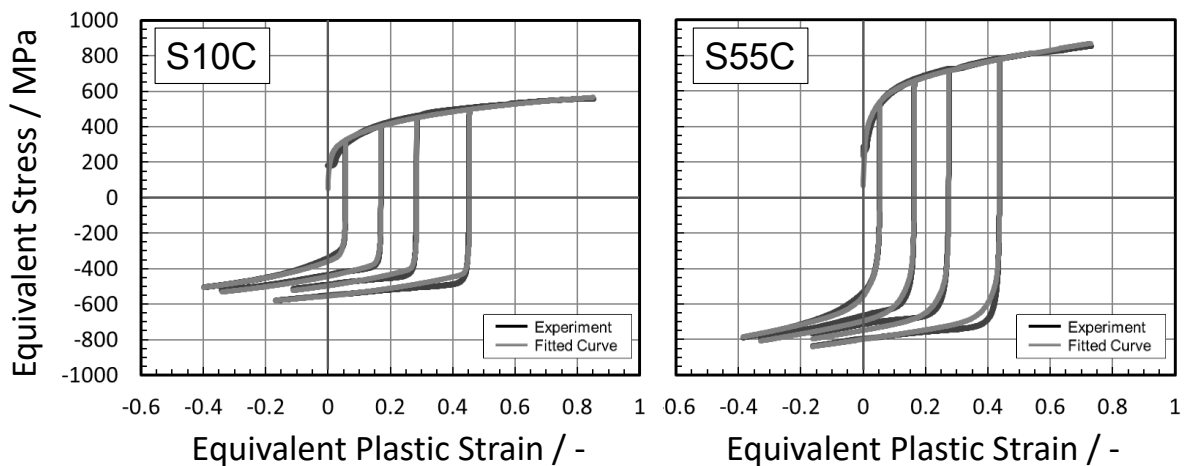


Figure 3: Stress–strain curves of S10C and S55C with fitted curves calculated using the Chaboche combined hardening model in Case 1

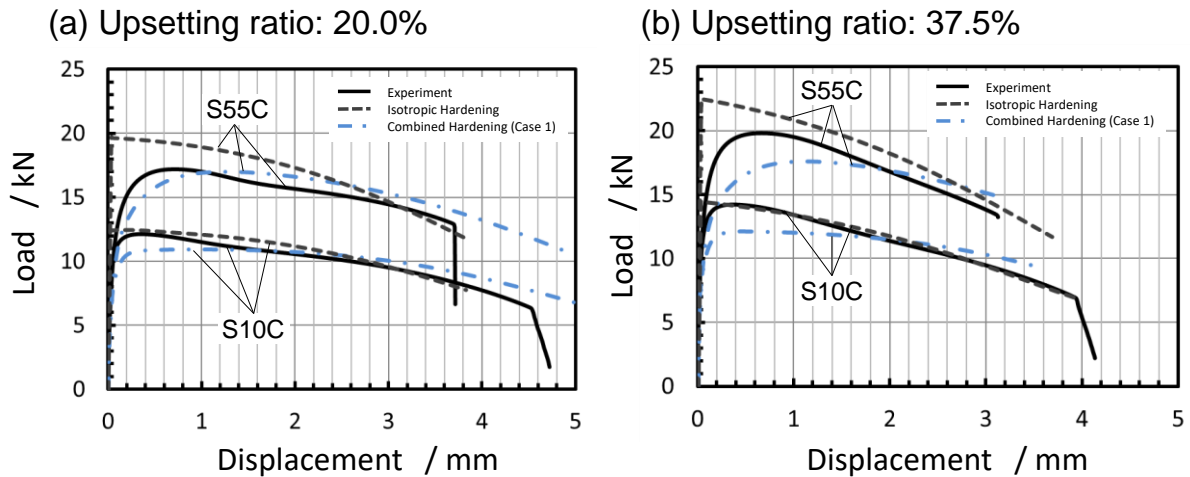


Figure 4: Load–displacement curves obtained from the experiments and FEA models of test (B) with the (a) 20.0%-upset and (b) 37.5%-upset specimens

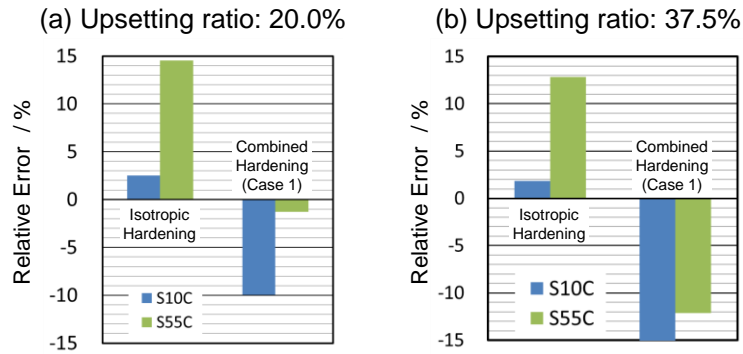


Figure 5: Relative errors of the calculated maximum load values with respect to the experimental values of test (B) in Case 1 with the (a) 20.0%-upset and (b) 37.5%-upset specimens

3.2 Parameter fitting to the reversed loading region of stress–strain curves (Case 2)

The strength of the upset specimens is noted to be underestimated in Case 1, along with a poor prediction accuracy. This is possibly because of the poor fits of the calculated stress–strain curves with respect to the experimental stress–strain curves in a strain range where the tensile specimens in test (B) are subjected to reversed loads, that is, a strain of ~ 0.23 and ~ 0.47 for the 20.0%-upset and 37.5%-upset specimens, respectively (Figure 3).

Therefore, the material parameters were reevaluated so that the calculated stress–strain curves were in agreement with the overall region of the stress–strain curves by weighting the range of strain where reversed loading occurred. Figures 6 and 9 show the recalculated equivalent stress–strain curves, along with the highlighted reversed loading regions of the stress–strain curves. The FEA model implemented using these parameters is referred to as Case 2.

The recalculated load–displacement curves from test (B) are shown in Figures 7 and 10 for the 20.0%-upset and 37.5%-upset specimens, respectively; the relative errors of the calculated maximum load values with respect to the experimental values in Case 2 are shown in Figures 8 and 11 for the 20.0%-upset and 37.5%-upset specimens, respectively. The strength of the upset specimens is also underestimated in Case 2, and the absolute values of relative errors of the maximum load in Case 2 are smaller than those in Case 1.

As mentioned earlier, simple shear tests can provide material parameters in a manner in which the stress–strain behavior can be reproduced over a range of strain where reversed loading occurs, and facilitate the accurate prediction of the strength of upset specimen.

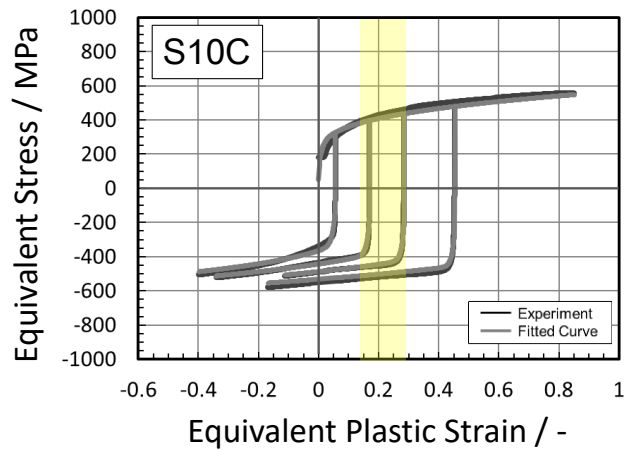


Figure 6: Stress–strain curves of S10C with fitted curves calculated using the Chaboche combined hardening model in Case 2 for predicting the strength of the 20.0%-upset specimens

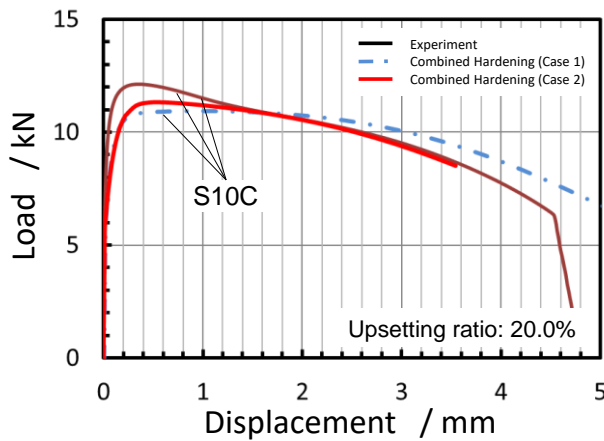


Figure 7: Load–displacement curves of S10C obtained from the experiments and FEA of test (B) using the 20.0%-upset specimens in Cases 1 and 2

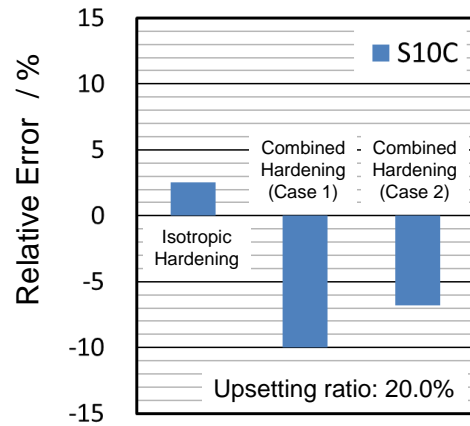


Figure 8: Relative errors of the calculated maximum load values with respect to the experimental values of test (B) using the 20.0%-upset specimens in Cases 1 and 2

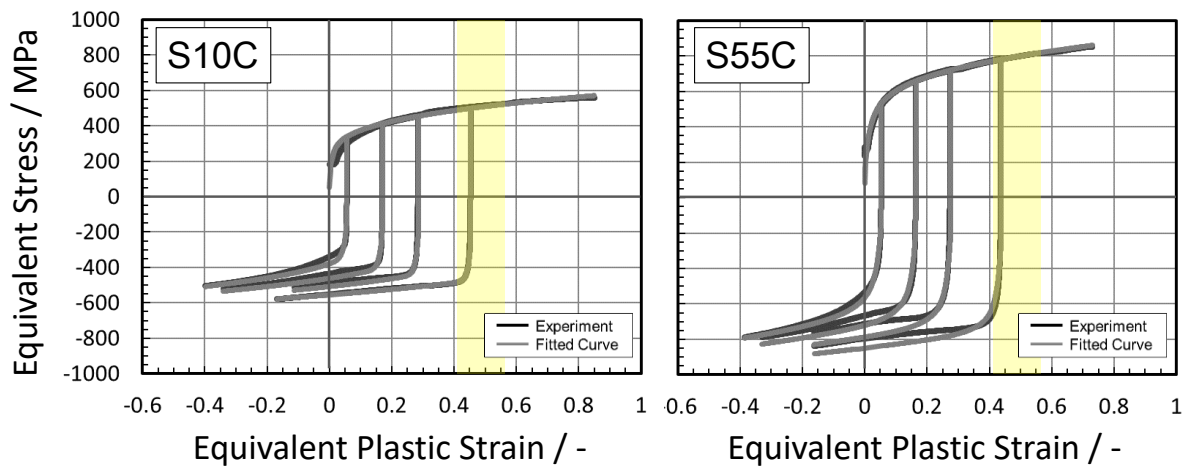


Figure 9: Stress–strain curves of S10C and S55C with fitted curves calculated using the Chaboche combined hardening model in Case 2 for predicting the strength of the 37.5%-upset specimens

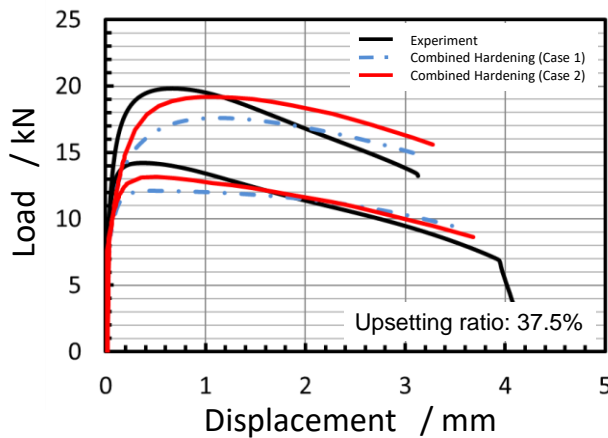


Figure 10: Load–displacement curves of S10C and S55C obtained from the experiments and FEA of test (B) using the 20.0%-upset specimens in Cases 1 and 2

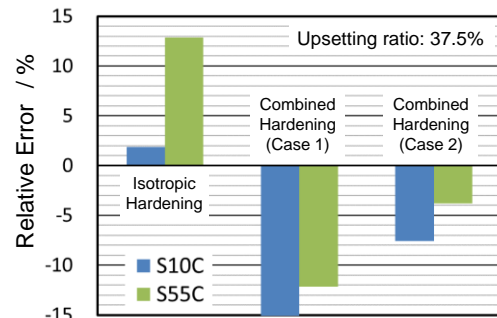


Figure 11: Relative errors of the calculated maximum load values with respect to the experimental values of test (B) using the 37.5%-upset specimens in Cases 1 and 2

4 CONCLUSIONS

A strength prediction method using a Chaboche combined hardening model was investigated in this study for predicting the strength of cold forged parts that are not subjected to heat treatment after cold forging. The highlights of the study are listed below:

- Stress–strain curves with reversed loading over a wide range of strains were obtained using simple shear tests.
- The strength of cold forged parts subjected to reversed loading was overestimated in the FEA model with isotropic hardening; therefore, it was inappropriate for predicting

the strength of these parts. However, the strength of the parts was underestimated in the FEA model with Chaboche combined hardening; this model could be considered to be appropriate.

- Simple shear tests assisted in identifying material parameters of the Chaboche combined hardening model by reproducing the stress–strain behavior over a range of strains where cold forged parts are subjected to reversed loads during operation, and enabled the accurate prediction of the strength of cold forged parts.

REFERENCES

- [1] Narita, S., Hayakawa, K., Kubota, Y., Harada, T., Uemori, T. Effect of Hardening Rule for Spring Back Behavior of Forging. *Procedia Eng. (ICTP 2017)* (2017) **207**: 167-172.
- [2] Chaboche, J.L. and Rousselier, G. On the plastic and viscoplastic constitutive equations - Part I: rules developed with internal variable concept. *J. Pressure Vessel Technol.* (1983) **105**: 153-158.
- [3] Suzuki, N., Hiwatashi, S., Uenishi, A., Kuwayama, T., Kuriyama, Y., Lemoine, X., Teodosiu, C. *J. Jpn. Soc. Technol. Plast. SOSEI-TO-KAKO.* (2005) **46**: 636-640.
- [4] Yoshikawa, N., Tamura, K., Kada, O. and Yoshida, T. *Proc. 68th JSTP Autumn Conference.* (2017): 149-150.
- [5] Shirakami, S., Tsunemi, Y., Yoshida, T. and Kuwabara, T. Work-hardening behaviour of sheet steels in large strain regions and its simple approximation. *J. Phys. Conf. Ser. (NUMISHEET 2018)* (2018) **1063**: 012107.